Scientific Reports

https://doi.org/10.1038/s41598-026-50178-x

Article in Press

# Multi-objective hybrid GA-PSO optimized PI control for grid-connected PV-fed cascaded H-bridge multilevel inverter

Received: 23 February 2026

Accepted: 20 April 2026

Published online: 27 April 2026

Cite this article as: Sharma B., Saxena V., Manna S. *et al.* Multi-objective hybrid GA-PSO optimized PI control for grid-connected PV-fed cascaded H-bridge multilevel inverter. *Sci Rep* (2026). https://doi.org/10.1038/s41598-026-50178-x

**Bhupender Sharma, Vivek Saxena, Saibal Manna, Pandry Narendra Rao, Mohammed H. Alsharif, Khalid Yahya & Mun-Kyeom Kim**

We are providing an unedited version of this manuscript to give early access to its findings. Before final publication, the manuscript will undergo further editing. Please note there may be errors present which affect the content, and all legal disclaimers apply.

If this paper is publishing under a Transparent Peer Review model then Peer Review reports will publish with the final article.

ARTICLE IN PRESS

© The Author(s) 2026. **Open Access** This article is licensed under a Creative Commons Attribution-NonCommercial-NoDerivatives 4.0 International License, which permits any non-commercial use, sharing, distribution and reproduction in any medium or format, as long as you give appropriate credit to the original author(s) and the source, provide a link to the Creative Commons licence, and indicate if you modified the licensed material. You do not have permission under this licence to share adapted material derived from this article or parts of it. The images or other third party material in this article are included in the article's Creative Commons licence, unless indicated otherwise in a credit line to the material. If material is not included in the article's Creative Commons licence and your intended use is not permitted by statutory regulation or exceeds the permitted use, you will need to obtain permission directly from the copyright holder. To view a copy of this licence, visit http://creativecommons.org/licenses/by-nc-nd/4.0/.

ARTICLE IN PRESS

# Multi-objective Hybrid GA-PSO optimized PI control for Grid-Connected PV-fed cascaded H-bridge multilevel inverter

Bhupender Sharma[1], Vivek Saxena[1], Saibal Manna[1], Pandry Narendra Rao[2], Mohammed H. Alsharif[3,*], Khalid Yahya[4], Mun-Kyeom Kim[5,*]

[1]Department of Electrical and Computer Engineering, ABES Engineering College,
Ghaziabad, UP, India; bhupender.sharma@abes.ac.in;
vivek.saxena@abes.ac.in, saibal.manna@gmail.com
[2]Department of Electrical and Electronics Engineering, R V College of Engineering, Bengaluru, Karnataka, India; pnrao@rvce.edu.in
[3]Department of AI Convergence Electronic Engineering, Sejong University, Seoul 05006, Korea; malsharif@sejong.ac.kr
[4]Department of Electrical and Engineering, Faculty of Engineering and Architecture, Istanbul Gelisim University, Istanbul, Turkey;
hayahya@gelisim.edu.tr
[5]School of Energy System Engineering, Chung-Ang University, 84 Heukseok-ro, Dongjak-gu, Seoul 06974, Republic of Korea; mkim@cau.ac.kr

**Corresponding author:** Mohammed H. Alsharif (malsharif@sejong.ac.kr); Mun-Kyeom Kim (mkim@cau.ac.kr)

***Abstract*—** The growing integration of PV energy systems into modern power grids necessitates advanced control techniques to maintain stable operation, fast dynamic response, and high-power quality under nonlinear and time-varying conditions. Cascaded H-bridge multilevel inverters (CHB-MLI) are widely adopted for grid-connected PV applications. This study develops a closed-loop control for a PV Integrated on-grid five-level CHB-MLI aimed at enhanced dynamic response and improved power quality. The hybrid GA-PSO technique is used for optimal tuning of PI controllers governing grid current regulation and DC-link voltage balancing through a multi-objective fitness function. The optimization framework simultaneously minimizes THD, DC-link voltage imbalance, steady state error and settling time. The simulation results are obtained by using MATLAB/Simulink, which demonstrates the feasibility of the proposed controller. Real-time validation using an OPAL-RT simulator further confirms the robustness and practical effectiveness of the hybrid GA-PSO-based PI control.

***Keywords*—***PV-integrated inverter, Hybrid GA-PSO, DC-link voltage balancing. PI controller optimization*

## I. Introduction

The rapid growth of PV energy systems has been driven by their clean energy generation, modularity, stability and declining installation costs. Grid-connected PV systems are increasingly deployed to meet renewable energy

ARTICLE IN PRESS

targets and reduce carbon emissions. Nevertheless, the variable nature of solar irradiance and nonlinear characteristics of power electronic interfaces pose significant challenges in achieving stable operation, high power quality and fast dynamic response under varying operating conditions [1]-[4]. MLI have become a preferred choice for medium and high power PV applications owing to its capability to enhance voltage waveform quality while limiting switching losses, harmonic distortion and reducing voltage stress on power semiconductor devices. Among various MLI topologies, the CHB-MLI is particularly suitable for PV-integrated systems because of its modular structure, stability, and independent DC sources and inherent fault tolerance. Unlike DC-MLI and FC-MLI topologies, CHB-MLI does not require clamping diodes or additional balancing capacitors, which simplifies the circuit configuration. These characteristics make CHB-MLI highly attractive for grid-connected PV applications, especially where multiple isolated DC sources are naturally available [5]-[12]. Despite the mentioned advantages, due to non-linear dynamics, voltage imbalance, and disturbances, the control of the MLI is very difficult. Generally, PI controllers are adopted for this purpose as they have simplified structures and implementations. Nevertheless, the parameters of fixed-gain PI controllers are typically tuned based on operating point and linearised model assumptions. When partial shading, disturbances or sudden changes occur, the performance of these controllers degrades significantly. This results in poor transient response and poor voltage balancing [13]-[16].

To mitigate the shortcomings of the tuning requirements of the traditional PI Controller, researchers have increasingly adopted different optimization approaches. GA have been widely investigated for determining controller parameters in MLI. GA enables efficient global exploration of the search space and can solve multi-objective problems easily without gradient information. Nevertheless, it is often associated with relatively high computational requirements and slow convergence. These factors can restrict its suitability for a PV-based system [17]-[18].

PSO has gained considerable attention for controller tuning due to its fast convergence, simple structure and reduced computational complexity. PSO-based PI controllers have demonstrated improved transient performance compared to classical PI tuning methods. Nevertheless, PSO exhibits weak global exploration capability and is highly sensitive to inertia weight and acceleration coefficients. Consequently, PSO-based controllers may converge to local optima and show degraded robustness under highly nonlinear and time-varying conditions in PV-fed CHB-MLI systems [19]-[21]. Current research highlights the potential of hybrid optimization techniques to overcome the shortcomings of individual GA and PSO algorithms. By integrating GA’s powerful global search capability with PSO’s rapid convergence and strong local refinement capability, hybrid GA-PSO algorithms can provide improved optimization performance [22]-[26]. Motivated by the above discussion, and based on the limitations identified in conventional PI-based controls, this research proposes a stability-oriented closed-loop control strategy that employs the GA-PSO technique for an on-grid 5-level CHB-MLI.

ARTICLE IN PRESS

The hybrid GA-PSO algorithm was adopted to combine the advantages of both optimization techniques. GA provides a strong global search capability, but may suffer from slow convergence, whereas PSO offers quick convergence but may become trapped in local optima. The hybrid approach integrates the exploration capability of GA with the exploitation capability of PSO, resulting in improved convergence speed and more reliable controller parameter optimization. By combining GA's effective global search capability with the quick convergence behaviour of PSO, the proposed controller achieves enhanced dynamic response, improved DC-link voltage balance under partial shading and reduced grid-current THD. Consequently, the proposed approach ensures superior stability and power quality transient performance compared to traditional PI-and standalone GA-tuned PI-controlled CHB-MLI systems operating under time-varying PV conditions. In this work, an sinusoidal phase-shifted pulse-width modulation (SPS-PWM) scheme is considered for CHB-MLI operation. The SPS-PWM is used to generate an accurate multilevel AC output waveform by maintaining the integrity of the reference voltage signals [8-11].

The present work investigates the dynamic behaviour of a CHB-MLI based PV system. The modelling framework is formulated in a generalized form so that it can be extended to MLI with different voltage levels. The proposed controller is validated through extensive simulation analysis and real-time testing using an OPAL-RT. Comparative results confirm superior dynamic performance, enhanced stability and improved robustness when compared with conventional PI, GA based-PI and PSO-based PI controllers.

The proposed system novelty is in its power transfer stability-oriented closed-loop architecture that enables independent and decoupled control of each HBC. Simultaneously, the proposed control scheme ensures the dc-link capacitor voltage is balanced even under variable conditions. The key novelty lies in the systematic multi-objective optimization of PI controller gains governing grid-current regulation and DC-link voltage balancing rather than relying on fixed tuned PI controllers.

## II. System architecture for grid-integrated PV sytem using Five-level CHB-MLI for hybrid control

A five-level CHB-MLI is employed in this work for grid-interfaced PV applications due to its modular structure, stability and superior power quality performance. The five-level CHB-MLI consists of two HBC connected in series per phase, each supplied by an isolated PV-fed DC-link source. By appropriate switching of two HBCs, the inverter generates five distinct voltage levels, enabling near sinusoidal output voltage synthesis. Compared to conventional two-level inverters, the five-level CHB-MLI significantly reduces output voltage THD. Compared to conventional two-level inverters, the five-level CHB-MLI significantly reduces output voltage harmonic distortion, dv/dt stress and switching losses while improving electromagnetic compatibility and grid current quality. These characteristics make the five-level CHB-MLI highly suitable for grid-connected PV systems, where multiple isolated DC sources are

naturally available, and strict grid code requirements must be satisfied. The block diagram of the proposed grid-integrated PV system comprises PV arrays supplying isolated DC-link voltages to individual HBCs, the cascaded stage, the grid interface filter and the control system is shown in Fig.1. Each PV array is connected to its own DC-DC boost converter. The Primary function of this stage is voltage boosting and isolation. MPPT ensures that the DC-DC converter constantly operates the corresponding PV array at its maximum power point. CHB-MLI is utilized to transform the DC power into the desired AC power. To obtain the desired voltage at the CHB-MLI output side, DC sources are synchronized with the help of the proposed controller. To achieve power flow balance under varying conditions, a closed-loop control scheme is implemented to regulate and maintain the DC bus voltage.

The control architecture employs a closed-loop grid-current controller to ensure accurate current tracking and UPF operation, along with a DC-link voltage control loop to maintain balanced voltage across the HBCs. To effectively handle the nonlinear dynamics, DC-link voltage imbalance, and operating uncertainties introduced by the partial shading and irradiance variations, a stability-oriented hybrid GA-PSO-based PI-control strategy is implemented. The hybrid controller optimally tunes the PI gains governing multi-objectives. Through coordinated control of the CHB-MLI output, the proposed hybrid approach enables reliable and high-performance grid integration of PV systems.

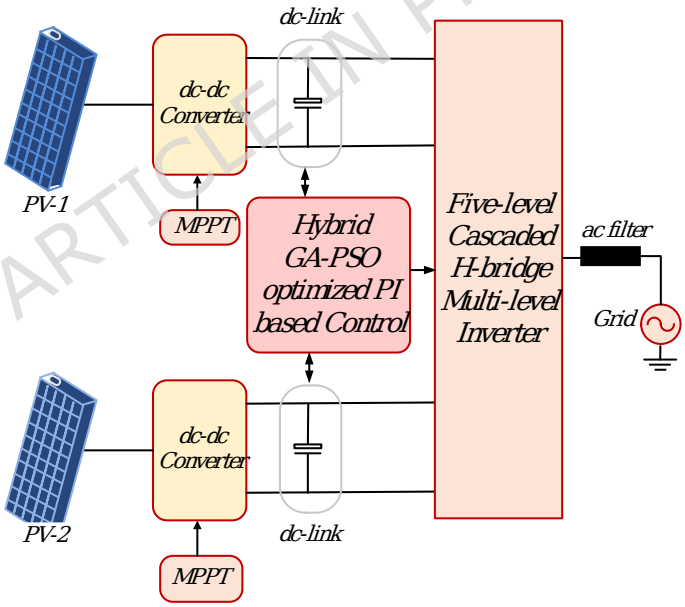



Fig. 1. Block Diagram for grid-integrated PV sytem using Five-level CHB-MLI for hybrid control

In the proposed grid-integrated PV system, each PV array is interfaced with the corresponding HBC through a DC-DC converter specifically designed to operate with an MPPT control mechanism. The primary role of this converter is to regulate the output voltage and ensure a stable DC-link voltage for each HBC despite partial shading. By decoupling the PV source dynamics from the inverter stage, the DC-DC converter enables independent control of the DC-link

ARTICLE IN PRESS

voltages, which is essential for continuously tracking the MPP of each PV array, thereby maximizing energy extraction and ensuring optimal utilization of the available solar power under conditions of uniform irradiance and partial shading. Furthermore, the use of individual DC-DC converters for each HBC enhances modularity and improves system robustness by allowing localized control of PV sources. This configuration significantly reduces DC-link voltage imbalance caused by mismatched PV conditions and shading effects, which are a critical challenge in CHB-MLI-based PV systems. The circuit diagram shown in Fig.2 illustrates a DC-DC boost converter being fed by two PV sources. The circuit consists of a PV source and the four primary components of a standard boost converter. The voltage produced by a PV array is not constant and will change depending on the intensity of sunlight and temperature. The DC-DC boost converter increases the low, variable DC voltage from the PV source to a higher, stable DC output voltage ($V_{dc1}$ and $V_{dc2}$) for the subsequent stages. This is achieved by the boost inductor storing energy when the high-frequency power switch is closed via a PWM signal. The diode acts as a one-way valve, ensuring the output current is directed only to the output capacitor. By rapidly cycling between two stages, the output voltage is boosted. The system under discussion uses a five-level CHB-MLI composed of two H-bridge cells, each powered by an independent, MPPT-controlled PV array subject to potentially different environmental conditions. To ensure the inverter model operates correctly, the power switches must be controlled to prevent the simultaneous turn-on of both switches in the same leg. The regulated DC-link voltages serve as inputs to the five-level CHB-MLI, while the inverter side hybrid GA-PSO optimized control ensures accurate grid current tracking and stable power injection into the grid. The coordinated operation of MPPT-controlled DC-DC converters and the hybrid CHB-MLI enables power conversion, improved dynamic response and high-quality grid-integration of the PV system.

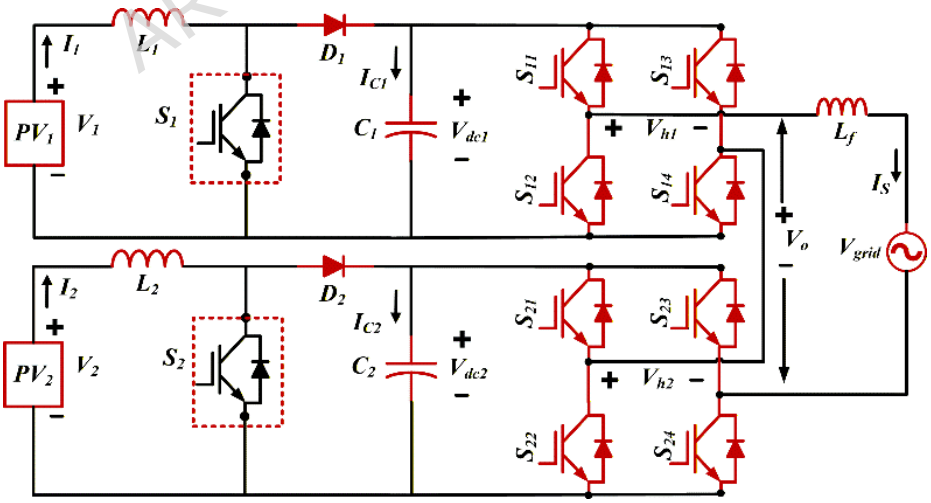



Fig. 2. Circuit Diagram of proposed grid-integated five-level CHB-MLI configuration

## III. Hybrid GA-PSO based controller optimization

In order to strengthen the dynamic behavior and operational robustness of PV-integrated on-grid CHB-MLI, a hybrid GA-PSO algorithm is adopted. The hybrid

ARTICLE IN PRESS

GA-PSO algorithm effectively combines the GA for comprehensive global search and PSO for rapid convergence and refined local exploitation, making it well-suited for nonlinear and multi-objective control problems encountered in CHB-MLI. This projected power transfer control scheme is designed to balance the DC-link capacitors within the HBC of the CHB-MLI, even when facing partial shading. Furthermore, the scheme allows for investigating two-way power flow and critically enables completely separate control for each HBC. This independent control provides flexible power extraction from the individual DC-links, ensuring capacitor voltage stabilization regardless of panel conflicts or environmental state. Essentially, the control system decouples the regulation of each HBC, allowing for different reference voltages to be applied to each cell. The block diagram of this control scheme is given in Fig.3. The control scheme's primary objectives are to ensure the DC-link capacitors are balanced within each HBC of the CHB-MLI, even when operating under partial shading or varying irradiation and temperature, which inherently causes uneven power injection into the individual HBCs, to reduce settling time, to achieve UPF operation while delivering a sinusoidal grid current with Low THD, to ensure maximum power is extracted from the SECS and that this is efficiently injected into the utility grid.

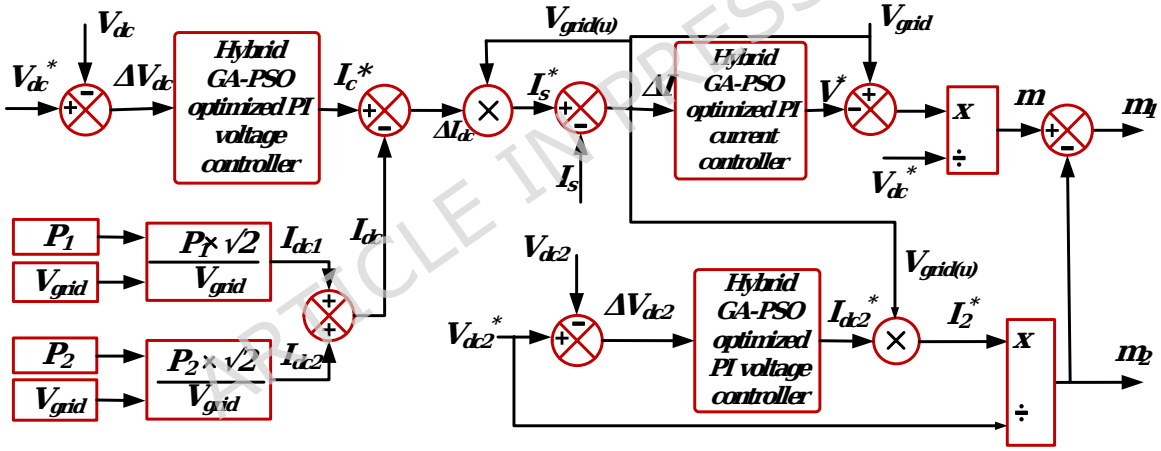



Fig. 3. Control Technique

In the proposed control, the total DC-link voltage of CHB-MLI is regulated by comparing the summed DC-link voltages with the reference values and processing the resulting error through a hybrid GA-PSO-optimized PI controller to generate reference capacitor current. The available PV power, determined through MPPT, is used to estimate the permissible grid current reference, ensuring that power injection does not exceed the instantaneous PV generation. The grid current error is then regulated through a hybrid GA-PSO-optimized current controller to produce the reference modulating signals. In addition, the individual dc-link voltage of each HBC is independently controlled using dedicated hybrid GA-PSO-optimized PI controllers to maintain voltage balance.

In Fig.3, the reference grid current is determined based on the instantaneous power available from the PV system. The MPPT controller DC-DC converter extracts the maximum available power from the PV arrays, which is used to estimate the permissible grid current reference. When PV generation

ARTICLE IN PRESS

decreases due to shading or environmental variations, the MPPT controller detects the reduction in available power and the control algorithm correspondingly reduces the reference grid current. This ensured that the inverter injects only the available PV power into the grid while maintaining stable DC-link voltage operation.

The synchronization among the MLI output current and the grid voltage is achieved using a grid voltage template that provides the phase information required to generate the reference grid current, ensuring that the MLI output current remains synchronized with the grid voltage and UPF. The DC-link voltage balancing is achieved through individual voltage control loops for each HBC. The measured capacitor voltages are evaluated against their corresponding reference values, and the resulting controller outputs are handled by PI controllers to regulate the capacitor charging and discharging process. Under partial shading and rapid irradiance variations, the MPPT algorithm continuously tracks the available PV power, and the controller dynamically adjusts the grid current reference accordingly. This coordinated control ensures stable DC-link voltage regulation even under varying operating conditions.

In the developed control approach, GA is initially used to generate a diverse population of candidate PI controller gain sets, thereby avoiding premature convergence and local minima. Subsequently, PSO is applied to the elite individuals obtained from the GA process to refine the solution using velocity and position updates. This cooperative optimization strategy significantly improves convergence speed and solution accuracy compared to standalone GA or PSO techniques. Hybrid GA-PSO is employed for optimal tuning of the PI controllers governing grid current regulation and DC voltage balancing. The optimization variables are defined as the P and I gain of the grid current controller and DC-link voltage controller expressed as:

$$X = K_{p,i}, K_{i,i}, K_{p,dc}, K_{i,dc} \quad (1)$$

Where $K_{p,i}$ and $K_{i,i}$ correspond to the grid current PI controller and $K_{p,dc}$ and $K_{i,dc}$ regulate the DC-link voltage balancing loop of the individual HBC. In the proposed control strategy, three PI control loops are used for the grid current control loop, the total DC-link voltage regulation loop and the individual capacitor balancing loop. The search ranges for the controller gains are selected based on preliminary stability analysis of the inverter control system and validated through initial simulation experiments to ensure stable convergence of the optimization process. These bounds ensure that optimization algorithm explores a sufficiently wide search space while maintaining the stable operation of the control system. The selected ranges are found to provide reliable convergence of the hybrid GA-PSO algorithm and improved controller performance. The bounds used for optimizations are:

$$K_{p,i} \in (0.01, 10), K_{i,i} \in (0.01, 500), K_{p,dc} \in (0.01, 10), K_{i,dc} \in (0.01, 500)$$

The hybrid GA-PSO minimizes the following multi-objective fitness function:

$$J = w_1.THD_i\ K_{i,i} + w_2.\Delta V_{dc} + w_{3.}\ e_i + w_{4.}\ t_s \quad (2)$$

Where $THD_i$ denotes grid current THD, $V_{dc}$ represents the dc-link voltage imbalance among HBC, $e_i$ is the steady state current tracking error and $t_s$ is the

ARTICLE IN PRESS

settling time. The weighting coefficients are selected as $w_1=0.4$, $w_2=0.3$, $w_3=0.2$, and $w_4=0.1$, prioritizing power quality and DC-link voltage stability.

The flowchart of the developed approach employed for optimal tuning of the PI controllers governing grid current regulation and DC voltage balancing is shown in Fig. 4. In the proposed approach, the GA stage is first used to perform a global exploration of the solution space to identify promising regions of the solution space. The candidate solutions represent the decision variables corresponding to the $K_p$ and $K_i$ of the PI controllers. The selection of parent chromosomes is performed using tournament selection. The crossover operation is implemented using arithmetic crossover. Gaussian mutation is applied to selected chromosomes with a small mutation probability. After which, the elite or best-performing chromosomes are transferred to the PSO stage to accelerate convergence. In this stage, each particle updates its velocity and position based on its personal solution and the global best solution. The algorithm concludes the optimization when either the maximum iteration count is reached or when the incremental improvement in the fitness function between consecutive iterations falls below a predefined tolerance value. The process is shown in the process flowchart in Fig. 4.

The mathematical expressions governing the proposed current reference generation, total DC-link voltage regulation, individual capacitor voltage regulation and modulation signal generation for SPS-PWM are summarized in the following equations (3)-(10).

Initially, the aggregate of measured dc voltages ($V_{dc}$) is evaluated against the reference value ($V_{dc}^*$). The corresponding voltage error ($\Delta V_{dc}$) is processed through a PI controller, to obtain the reference capacitor current ($I_c^*$).

$$V_{dc}=V_{dc1}+V_{dc2} \tag{3}$$

The reference current ($I_c^*$) is given by:

$$I_c^*(t)=k_{p1}\Delta V_{dc}(t)+k_{i1}\int \Delta V_{dc}(t)\,dt \tag{4}$$

The coefficients '$k_{p1}$' and '$k_{i1}$' corresponds to the gain of voltage PI controller. The current extracted from the PV array, depending on the prevailing conditions is '$I_{dc}$', and its instantaneous value is given by the following expression:

$$I_{dc}(t)=\sqrt{2}\left(\frac{P_{PV1}+P_{PV2}}{V_{grid,rms}}\right) \tag{5}$$

Considering, the power required to sustain capacitor voltages at their desired reference levels, the instantaneous total current available for the CHB-MLI is determined as:

$$\Delta I_{dc}(t)=\left(k_{p1}.\Delta V_{dc}(t)+k_{i1}\int \Delta V_{dc}(t)\,dt\right)-\sqrt{2}\left(\frac{P_{PV1}+P_{PV2}}{V_{grid,rms}}\right) \tag{6}$$

Subsequently, the control framework aligns the MLI ac side current with the grid voltage, while maintain UPF by employing the unit template of grid voltage. As a result, reference ac side current ($I_s^*$) is generated, and its instant value is given in the equation:

ARTICLE IN PRESS

$$I_s^*(t) = \left(k_{p1}.\Delta V_{dc}(t) + k_{i1}\int \Delta V_{dc}(t)\,dt\right) - \sqrt{2}\left(\frac{P_{PV1}+P_{PV2}}{V_{grid,rms}}\right)\sin(\omega t) \quad (7)$$

The current ($I_s^*$) is compared with the grid current ($I_s$) as shown in Fig.3 and the resultant current ($\Delta I$) is fed to the hybrid GA-PSO optimized PI current controller. Similarly, the controller produces a reference component of ac voltage ($V^*$).

$$V^*(t) = k_{p2}.\Delta V(t) \quad (8)$$

Where '$k_{p2}$' is the proportionality constant of the lower controller.

In the final stage of the proposed control framework, the '$V_{dc1}$' is regulated to its reference voltage by subtracting the generated reference modulation functions '$m_2$' from the generated reference voltage modulation signal '$m_1$'. Lower HBC is independently regulated by comparing its dc-link capacitor voltage with its reference values ($V_{dc2}^*$). The resultant '$\Delta V_{dc2}$' is then processed by a PI controller in the subsequent stage. The reference dc current component '$I_{dc2}^*$' and its instant value of current ($I_2^*$) are generated as shown in Fig.3.

$$I_{dc2}^*(t) = k_{p3}\Delta V_{dc2}(t) + k_{i3}\int \Delta V_{dc2}(t)\,dt \quad (9)$$

$$I_2^*(t) = \left(k_{p3}\Delta V_{dc2}(t) + k_{i3}\int \Delta V_{dc2}(t)\,dt\right)\sin(\omega t) \quad (10)$$

After obtaining the optimal PI controller gains using the proposed hybrid GA-PSO algorithms framework, the controller outputs are utilized to generate the reference modulating signals for the inverter switches. These reference signals are processed through a SPS-PWM, where they are continuously compared with multiple carrier signals to synthesize the desired five-level output voltage waveform. The proposed system uses the SPS-PWM technique to generate the firing signals for the CHB-MLI, which is achieved by feeding closed-loop-controlled modulating signals into the PWM block, as shown in Fig.5.

ARTICLE IN PRESS

ARTICLE IN PRESS

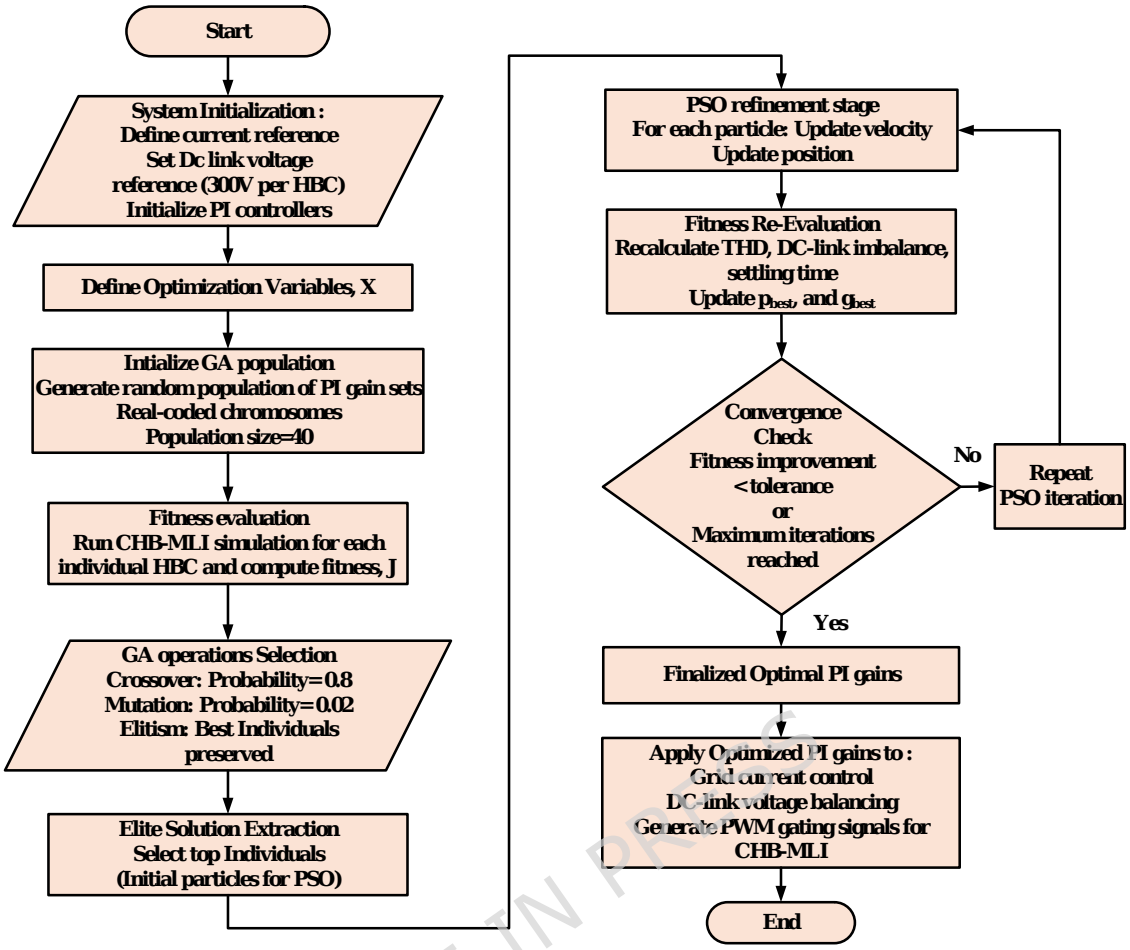



Fig.4 - Flowchart of Hybrid GA-PSO for optimal tuning of the PI controllers governing grid current regulation and DC voltage balancing

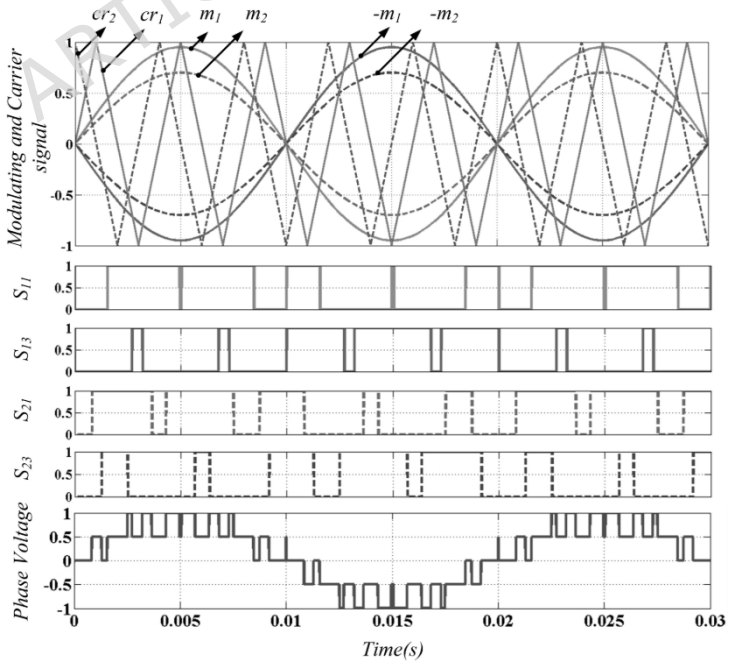



Fig. 5. SPS-PWM Switching Strategy

ARTICLE IN PRESS

## IV. **Simulation Results and Analysis**

The effectiveness of the proposed hybrid GA-PSO-based PI control strategy for the PV-integrated on-grid 5-level CHB-MLI is evaluated through detailed MATLAB/Simulink simulations. The results are compared with a conventional fixed gain PI controller under identical operating conditions to highlight improvements in dynamic response, DC-link voltage balancing and grid current harmonic performance. The proposed approach is modelled, and its results are validated. The performance of the CHB-MLI-based SECS was simulated and tested under steady state conditions using specific parameters to achieve UPF, enhanced dynamic response, harmonic elimination, and DC-link capacitor balancing despite panel mismatching. Uneven power input demonstrates the panel mismatch by showing the two PV string currents ($I_1$ and $I_2$). The current difference leads to uneven DC-link capacitor voltage unbalance. The main goal of the controller is to successfully balance these DC-link capacitor voltages even with varying PV power levels, while also injecting a sinusoidal grid current. Table I represents the simulation parameters used in the study and Table II shows the parameters used for Hybrid GA-PSO for optimization in the study. The DC-link reference voltage of 300V per HBC was selected to ensure stable inverter operation for a 230V (rms) grid system. Since the peak grid voltage is approximately 325V, the cascaded configuration of two HBC provides a total DC-link voltage of 600V. This voltage level provides sufficient margin for stable SPWM modulation, accurate grid current control, and reliable power injection into the grid while maintaining acceptable voltage stress on the switching devices.

The GA-PSO parameters were selected based on commonly recommended values in evolutionary optimization literature and validated through preliminary simulation studies. The justification for the parameters used for control optimization for Hybrid GA-PSO is mentioned in Table II.

ARTICLE IN PRESS

Table I: Simulation parameters

| **Parameter** | **Value in simulation** |
|---|---|
| Individual capacitor DC link voltage | 300 V |
| DC bus capacitance | 3000 µF |
| PWM switching frequency | 2.5 kHz |
| Grid frequency | 50 Hz |
| Single-phase Grid Voltage | 230V (RMS) |
| No. of HBC | 02 |
| PI current controller gains | Optimized via Hybrid GA-PSO |
| PI DC-link controller gains | Optimized via Hybrid GA-PSO |
| Solar irradiance | 600-1000 W/m$^2$ |
| Simulation step size | 1e-6 s |

ARTICLE IN PRESS

| | |
|---|---|
| Filter inductance and resistance | 3 mH & 0.2 ohms |
| | |

Table II: Hybrid GA-PSO parameters used for control optimization

| **Parameter** | **Value** | **Justification** |
|---|---|---|
| Population size | 40 | Ensures solution diversity |
| Maximum Generations | 60 | Reduced due to PSO acceleration |
| GA crossover probability | 0.8 | Effective genetic mixing |
| GA mutation probability | 0.02 | Avoids premature convergence |
| PSO inertia weight (w) | 0.7- 0.4 | Balances exploration-exploitation |
| Cognitive coefficients ($c_1$) | 1.5 | Individual learning |
| Social coefficient ($c_2$) | 1.5 | Global learning |
| Elite particles | 5 | Best GA solutions refined by PSO |
| Encoding | Real-coded | Suitable for controller gains |

***(a) Grid-current quality and THD analysis***

Single-phase output voltage and current of MLI, which is connected to single-phase grid is shown above in Fig.6 and the zoomed view of the above fig. is given in the same fig. The fig. clearly shows that the output current and voltage is sinusoidal in nature. Fig.6, illustrates the grid current waveform and the corresponding harmonic spectrum is shown in Fig. 8. It is evident that with the proposed controller, the grid current waveform becomes significantly smoother and more sinusoidal. UPF and sinusoidal current plots the $V_{grid}$ and the $I_s$. Fig.6, confirms that the voltage and current are sunchronized in phase, verifying UPF operation as intended by the control scheme. Furthermore, the $I_s$ is highly sinusoidal, achieving a low THD. The grid current THD is reduced from 4.8% in the conventional PI control case to around 2.08% and, corresponding to a reduction in THD. This improvement ensures compliance with IEEE harmonic standards and validates the performance of the multi-objective optimization approach in enhancing power quality. Fig. 7 and Fig. 9 shows that CHB-MLI output current and voltage THDs are 2.08% and 1.08%, respectively. Both the THDs are within the limited range of 5% and have better power quality.

ARTICLE IN PRESS

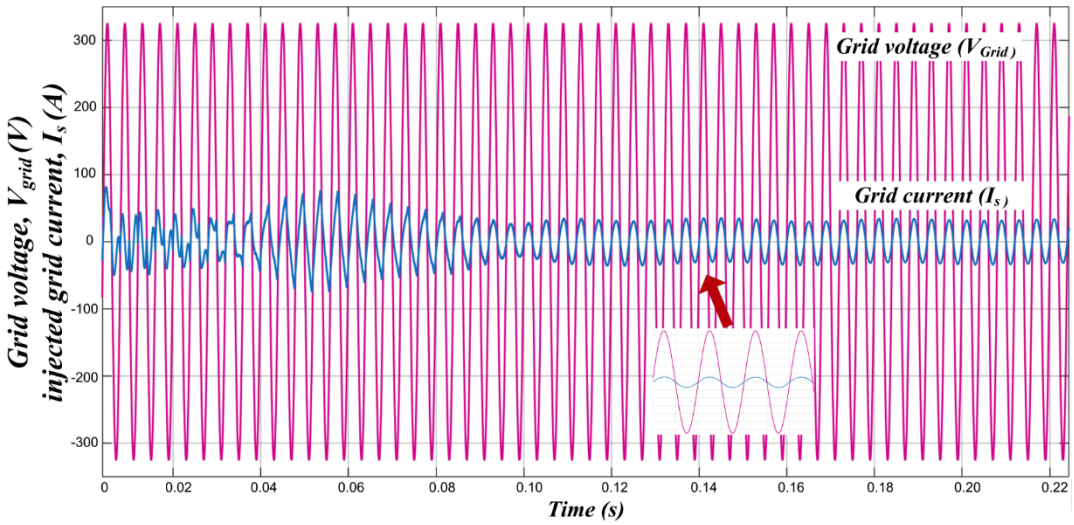



Fig. 6. Single-phase grid voltage ($V_s$) and injected grid current ($I_s$)

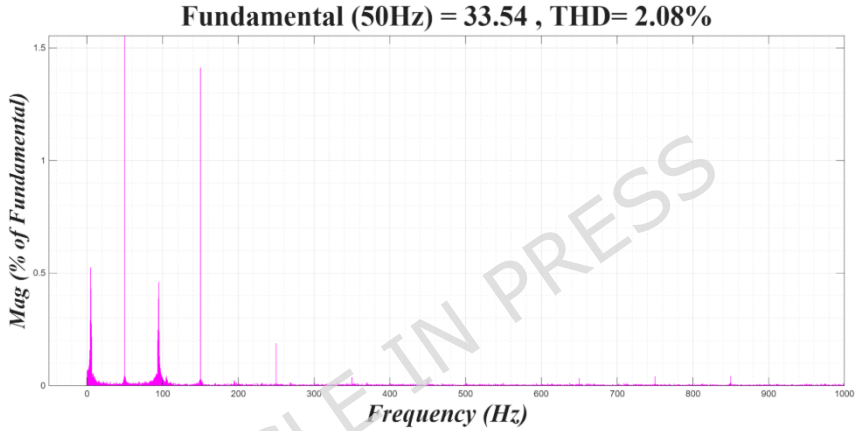



Fig. 7. Injected grid Current THD

### *(b) Five-level inverter operation*

Voltage levels display the 3-level output voltages of each of the HBC. Since the two HBCs are connected in cascade, their outputs combine to produce a five-level voltage at the overall CHB-MLI output ($V_{ac}$) waveform as given in Fig. 8, which justifies the proper five-level inverter operation. The generation of well-defined voltage levels demonstrates the hybrid GA-PSO optimized PI controllers and the modulation strategy. This balanced five-level operation contributes to minimized power devices voltage stress, improved waveform quality and lower grid current THD, thereby validating the capability of the developed controller.

ARTICLE IN PRESS

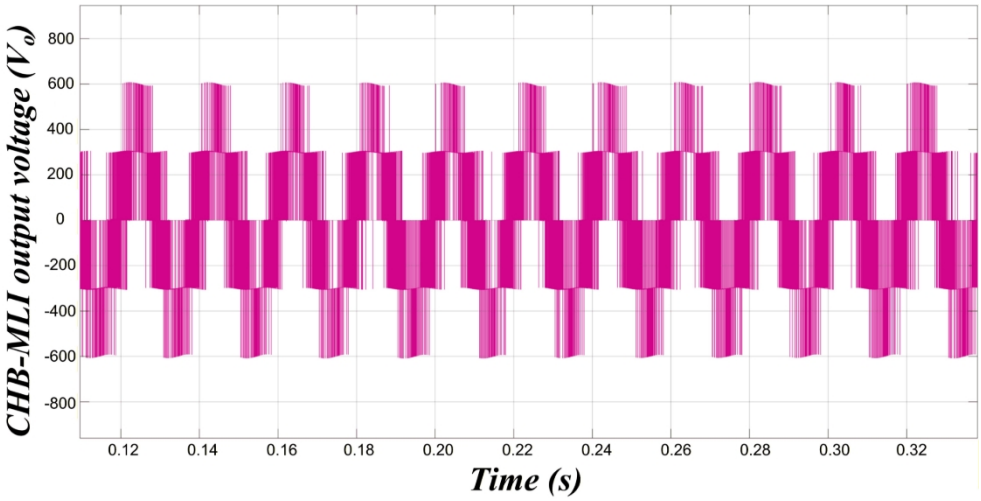



Fig. 8. Five-level CHB-MLI output voltage

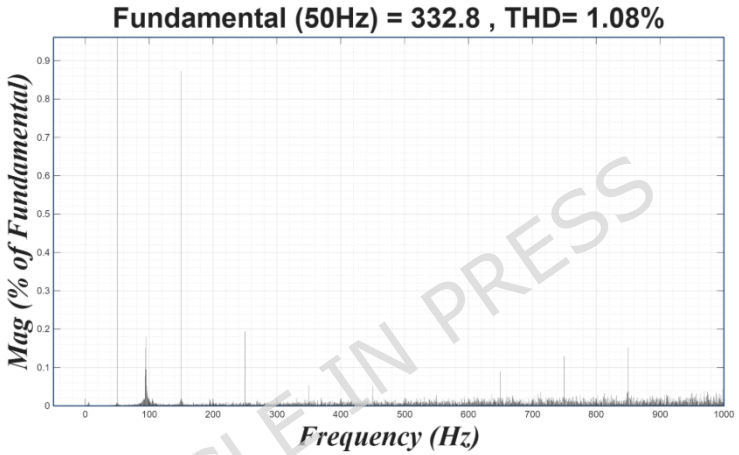



Fig. 9. CHBMLI output voltage THD

***(c) DC-link voltage balancing performance***

The DC-link capacitor voltage profiles of the individual HBC under partial shading conditions are shown in Fig. The chopper control technique used to monitor or control each HBC independently successfully achieves the capacitor balance target. The proposed GA-PSO based controller effectively maintains balanced DC-link voltages across the HBC. The DC-link voltage deviation is limited to below 2-3%, representing an improvement as compared to classical PI controllers. The voltage controllers within the respective HBC control schemes effectively stabilize the voltages. It is clearly demonstrated in Fig.10 that despite the panel mismatch, the capacitors $C_1$ and $C_2$ are balanced within a permitted timeframe. This enhanced balancing capability contributes to improved inverter reliability and stable multilevel voltage synthesis.

***(d) Dynamic response under irradiance variations***

To evaluate the dynamic performance, step changes in solar irradiance conditions are applied to the system. The proposed controller achieves a significantly faster response, reducing the settling time to around 0.11s as shown in Fig. 10, while the conventional PI controller exhibits a slower response. The enhanced transient behavior is primarily due to hybrid GA-PSO

optimization, which ensures appropriate proportional and integral selection gain for both current control and DC-link voltage regulation.

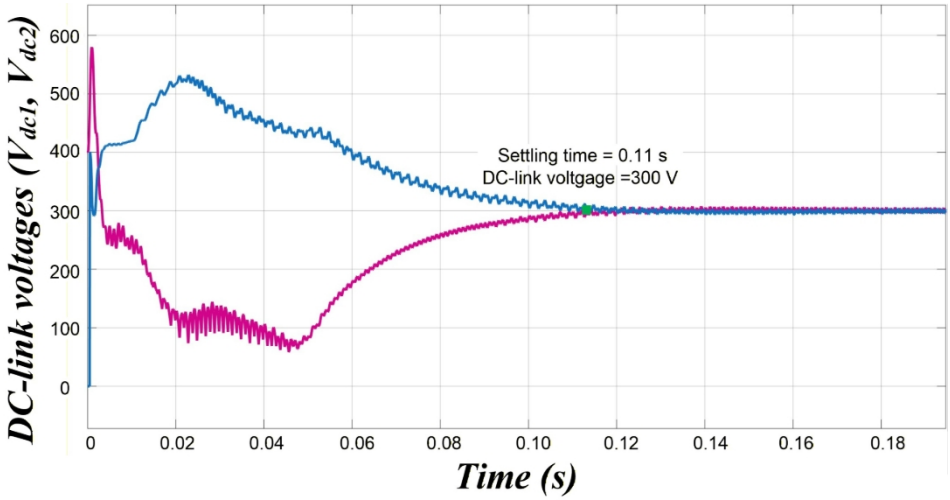



Fig. 10. DC link capacitor voltages

### *(e) Real-time validation using OPAL-RT simulator*

To further demonstrate the practical applicability of the proposed hybrid control, real-time simulation studies are performed using a real-time simulator. The developed PV-integrated on-grid five-level CHB-MLI model, along with the optimized control algorithm, is implemented in a real-time environment to investigate its behavior under dynamic operating conditions. The real-time results closely match the MATLA/Simulink outcomes, confirming consistent grid-current tracking, effective DC-link voltage balancing, and stable five-level inverter operation in Fig. 11, 12, 13 and 14 respectively. Moreover, the proposed controller demonstrates superior dynamic response and robustness during irradiance and load transients when compared to conventional PI. These results validate the real-time feasibility and practical adaptability of the designed control approach for taken system.

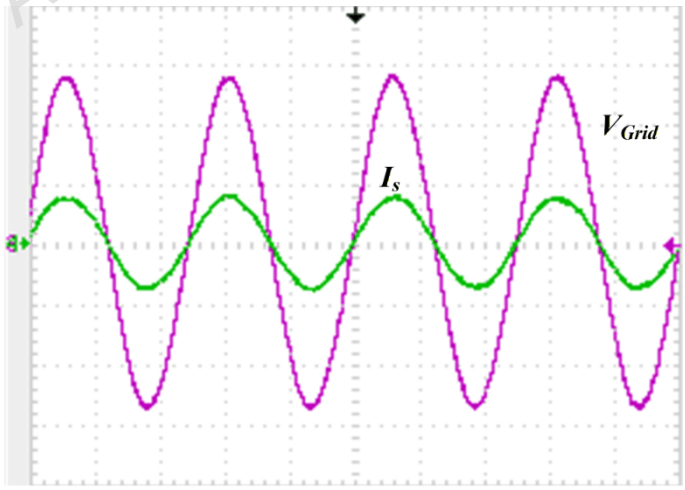



Fig. 11. OPAL-RT real-time simulator result for consistent grid-current tracking

ARTICLE IN PRESS

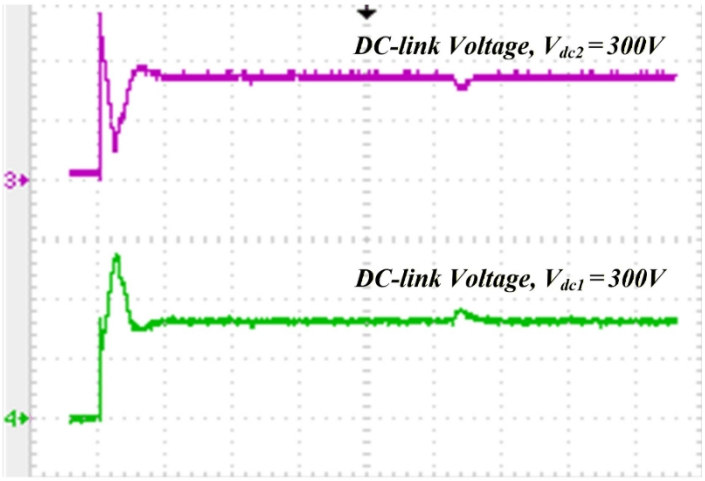



Fig. 12. OPAL-RT real-time simulator result for effective DC-link voltage balancing

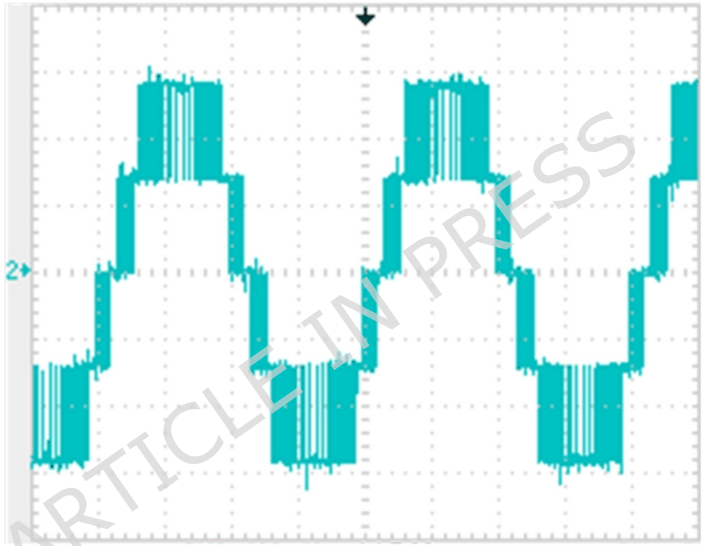
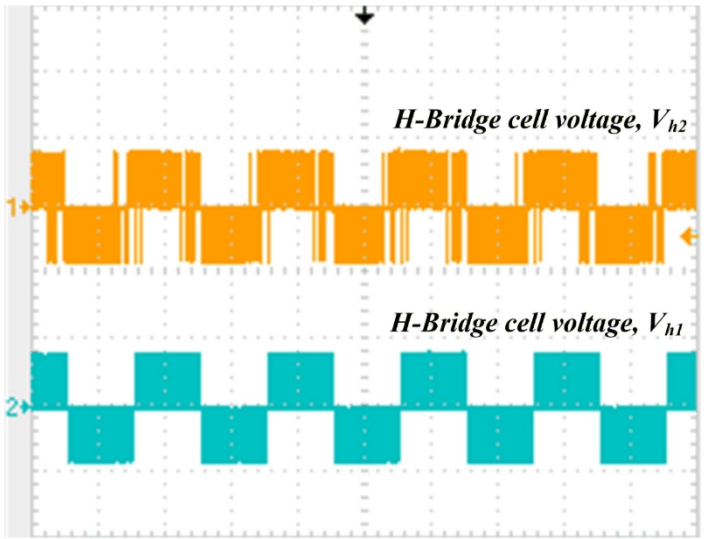



Fig. 13. OPAL-RT real-time simulator result for stable five-level CHB-MLI operation



ARTICLE IN PRESS

Fig 14. OPAL-RT real-time simulator result for individual HBC output voltage

***(f) Discussion on control effectiveness***

The obtained results clearly demonstrate that the proposed control strategy outperforms the conventional PI controller in all key performance metrics. The integration of GA and PSO enables effective global exploration and fast local exploitation during the optimization process, leading to superior gain selection compared to trial and error tuning. Moreover, the improved robustness under partial shading and irradiance variations highlights the suitability of the proposed approach for practical PV-integrated on-grid CHB-MLI applications.

The main improvements include reduced grid current THD, improved DC-link voltage balancing among CHB cells, faster dynamic response during irradiance changes, and enhanced system robustness under varying operation conditions. The achieved improvements in THD reduction, DC-link voltage balancing and dynamic response collectively validate the stability-oriented design philosophy of the developed controller.

To evaluate the robustness of the optimization process, the hybrid GA-PSO algorithm was executed for multiple independent runs with different initial populations. The obtained controller parameters showed minimal variation between runs, indicating consistent convergence behavior. The reported results correspond to the best converged solution obtained across these runs. Table III shows the performance assessment of the proposed controller against the available different control strategies.

Table-III Performance comparison of different control strategies

| **Control Strategy** | **Grid-current THD (%)** | **DC-link voltage imbalance (%)** | **Settling time** | **Key remarks** | **References** |
|---|---|---|---|---|---|
| Conventional PI | 4.5-5.0 | >5 | 0.19 | Fixed gain, Limited robustness | [27] |
| GA optimized PI | 3-3.5 | 3.5- 4.0 | 0.15 | Improved power quality, slow convergence | [17] |
| PSO optimized PI | 2.8-3.0 | 3.0-3.5 | 0.13 | Fast convergence, risk of local minima | [28], [29] |
| Hybrid GA-PSO PI (Proposed) | 2.08 | < 2 | 0.11 | Best Dynamic response and robustness | In this work |

ARTICLE IN PRESS

## V. Conclusion

This paper proposes a grid-connected five-level CHB-MLI for converting power from a PV in SECS into AC power for grid injection. The proposed approach systematically optimizes the PI controller gains governing multi-objective framework thereby addressing the limitations of conventional fixed gain PI control under time varying operation conditions. The core achievement is the successful implementation of a control scheme that ensures the maximum possible power is extracted from each individual HBC at all times, even under conditions of partial shading and panel mismatch. Crucially, the authors met their main goal by attaining the target balanced DC-Link voltage of 300V at both HBCs, despite the unequal PV input parameters. This topology significantly improves the utilization of individually connected PV strings, each equipped with its own independent boost converter and MPPT system. Simulation results confirm that the control technique effectively achieves DC-link capacitor voltage balancing (imbalances below 2%) and injects a sinusoidal grid current with low current THD of 2.08% and UPF. In conclusion, the presented on-grid PV converter topology and its stability-oriented closed loop control technique offer a robust and efficient solution to realize the critical objectives of DC capacitor voltage balancing and high-power quality. Subsequent research will wmphasize on experimental hardware implementation and extension of the proposed approach to higher level multilevel configurations.

## Author Contributions

**Concepts:** Bhupender Sharma and Vivek Saxena; **Methodology:** Bhupender Sharma, Saibal Manna, Mohammed H. Alsharif, Mun-Kyeom Kim; **Writing-Original Draft Preparation**: Bhupender Sharma, Vivek Saxena, Saibal Manna; **Writing-Final Review and Editing**: Mohammed H. Alsharif, Khalid Yahya, Mun-Kyeom Kim; **Project Administration:** Mohammed H. Alsharif & Khalid Yahya; **Funding Acquisition:** Mun-Kyeom Kim.

## Data Availability Statement

The datasets used and analyzed during the research are available from the corresponding author on the request.

## Funding

This work was supported by the National Research Foundation of Korea (NRF) grant funded by the Korea government (MSIT) (Grant Number:RS-2026-25484700).

## Human and Animal Rights

It does not contain any studies with human participants or animals performed by any of the authors.

## Competing Interest

The authors declare that there is no conflict of interest.

## References

[1] Öztürk, S. & Çadırcı, I. A Generalized and Flexible Control Scheme for Photovoltaic Grid-Tie Microinverters," in IEEE Transactions on Industry Applications, vol. 54, no. 1, pp. 505-516. doi: 10.1109/TIA.2017.2753175. (2018).

[2] M. H. Alsharif, "Optimization design and economic analysis of energy management strategy based on photovoltaic/energy storage for heterogeneous

ARTICLE IN PRESS

cellular networks using the HOMER model," Solar Energy, vol. 147, p. 133-150, 2017.

[3] Raghava Sharma, P V V, & Neelshetty, K. Novel cascaded tilt fractional-order integral derivative with a proportional integral for harmonics mitigation in 31-level multi-level inverter. Computers and Electrical Engineering, 123, 110280. https://doi.org/10.1016/j.compeleceng.2025.110280 (2025).

[4] Minh, C. L. T., & Duong, M. Q. Reducing Overall Active Power Loss by Placing Solar and Wind Generators in a Distribution Power System using Wild Horse Optimizer Algorithm. *Journal of Engineering and Technological Sciences*, *56*(5), 571–582.
https://doi.org/10.5614/j.eng.technol.sci.2024.56.5.2 (2024).

[5] Kouro, S. et Al. Recent advances and industrial applications of multilevel converters. IEEE Transaction on Industrial Electronics, 57, 2553-2580. doi: 10.1109/TIE.2010.2049719 (2010).

[6] Kumar, N.B., M, U.M.R., Lakshminarayana, P. et al. Performance measurement of high gain Landsman converter with ANFIS based MPPT and cascaded H-bridge thirty-one multilevel inverter in a single-phase grid-connected PV system. Sci Rep **15**, 45295. https://doi.org/10.1038/s41598-025-28943-1(2025).

[7] M. H. Alsharif, R. Nordin, M. Ismail, "Green wireless network optimisation strategies within smart grid environments for Long Term Evolution (LTE) cellular networks in Malaysia," Renewable Energy, vol. 85, p. 157-170, 2016.

[8] Alexander, SA. Development of solar photovoltaic inverter with reduced harmonic distortions suitable for Indian sub-continent. Renewable and Sustainable Energy Reviews, (56), 694–704. https://doi.org/10.1016/j.rser.2015.11.092 (2016).

[9] Sharma,B., Manna, S., Saxena,V., et al. A comprehensive review of multi-level inverters, modulation, and control for grid-interfaced solar PV systems. Scientific Reports 15, 661. https://doi.org/10.1038/s41598-024-84296-1 (2025).

[10] Rodríguez, J., Lai, JS. & Peng,FZ. Multilevel inverters: A survey of topologies, controls, and applications. IEEE Transactions on Industrial Electronics, 49, 724–738. https://doi.org/10.1109/TIE.2002.801052 (2002).

[11] Sinha,A ., Jana K. Chandra & M DAS Kumar. An inclusive review on different multi-level inverter topologies, their modulation and control strategies for a grid-connected photo-voltaic system. Solar Energy, 170, 633–57. https://doi.org/10.1016/j.solener.2018.06.001 (2018).

[12] Behera, R.R., Dash, A.R., Mishra, S. *et al.* Implementation of a hybrid neural network control technique to a cascaded MLI based SAPF. *Sci Rep* **14**, 8614 https://doi.org/10.1038/s41598-024-58137-0 (2024).

[13] Kouser, S., Dheep, G.R. & Bansal, R.C. Artificial Ecosystem Optimization Algorithm Tuned PI-Controlled Grid-connected PV System. Smart Grids and Energy **10**, 25. https://doi.org/10.1007/s40866-025-00251-7 (2025).

[14] Mohamed, M.A.E., Ward, S.A., El-Gohary, M.F. *et al.* Hybrid fuzzy logic–PI control with metaheuristic optimization for enhanced performance of high-penetration grid-connected PV systems. *Sci Rep* **15**, 24650 https://doi.org/10.1038/s41598-025-09336-w. (2025).

[15] M. H. Alsharif, "Comparative analysis of solar-powered base stations for green mobile networks," Energies, vol. 10, no. 8, p. 1208, 2017.

[16] Siham Chakiri, Youssef Mchaouar, Younes Abouelmahjoub, Hassan Abouobaida, & Fouad Giri. Advanced Adaptive Control and Formal Stability Analysis of the N-Level Cascaded H-Bridge Multilevel Inverter fed Single-Stage Grid-Tied PV System Applications with an LCL Filter. Computers and Electrical Engineering, 126, 11053. https://doi.org/10.1016/j.compeleceng (2025).

ARTICLE IN PRESS

[17] Slowik, A., Kwasnicka, H. Evolutionary algorithms and their applications to engineering problems. Neural Comput & Applic **32**, 12363–12379. https://doi.org/10.1007/s00521-020-04832-8 (2020).
[18] Nasser, A.M., Refky, A., Shatla, H. *et al.* A grey wolf optimization-based modified SPWM control scheme for a three-phase half bridge cascaded multilevel inverter. *Sci Rep* **14**, 7016. https://doi.org/10.1038/s41598-024-57262-0 (2024).
[19] Sahoo, S. & Singh, B. GA-based control of grid-connected converters under dynamic conditions. IEEE Transaction on Sustainable Energy, 13, 45-56. (2022).
[20] Xiao, W., Wang, D., Xie, F. et al. Improved global fast terminal sliding mode control-based MPPT method for photovoltaic systems. J. Power Electron. **25**, 1605–1614. https://doi.org/10.1007/s43236-025-01009-1 (2025).
[21] Alamgir Hossain,M. Roy Pota,R. Squartini,S. & Fathi Abdou.,A. Modified PSO algorithm for real-time energy management in grid-connected microgrids. Renewable Energy, 136, 746-757. https://doi.org/10.1016/j.renene.2019.01.005. (2019).
[22] Roslan MF, Al-Shetwi AQ, Hannan MA, Ker PJ, Zuhdi AWM. Particle swarm optimization algorithm-based PI inverter controller for a grid-connected PV system. PLOS ONE 16(10): e0259358. https://doi.org/10.1371/journal.pone.0259358 (2021)
[23] UrgUn, S.; Yigit, H.; Mirjalili, S. Investigation of Recent Metaheuristics Based Selective Harmonic Elimination Problem for Different Levels of Multilevel Inverters. Electronics, 12, 1058. https://doi.org/10.3390/electronics12041058 (2023).
[24] Arulkumar, S., Arif, M., Patro, P. et al. GrCRA PCRTAM net based hybrid approach for intelligent control and optimal power management in renewable integrated power distribution systems. Sci Rep 15, 39976. https://doi.org/10.1038/s41598-025-23793-3 (2025).
[25] Marzuki, M.H., Ramlan, N.H., Ab-Ghani, S., Nasir, N.M., Norazman, M.A.I. (2024). Performance Analysis of GA and PSO Based PI Controller for Cascaded H-bridge Multilevel Inverter Output Voltage Regulation. In: Md. Zain, Z., Sulaiman, N., Mustafa, M., Shakib, M.N., A. Jabbar, W. (eds) Proceedings of the 7th International Conference on Electrical, Control and Computer Engineering—Volume 2. InECCE . Lecture Notes in Electrical Engineering, vol 1213. Springer, Singapore. https://doi.org/10.1007/978-981-97-3851-9_21 (2023).
[26] Kumar, P., Arya, SR., Mistry, KD. & Giri, AK. Hybrid self-learning controller for restoration of voltage power quality using optimized multilayer neural network. International Journal of Circuit Theory and Applications, 49 :4248–4273. https://doi.org/10.1002/cta.3084 (2021).
[27] Kazmierkowski,M. P. & Malesani, L. Current control techniques for three-phase voltage-source PWM converters: a survey. IEEE Transactions on Industrial Electronics, vol. 45, no. 5, pp. 691-703, doi: 10.1109/41.720325 (1998).
[28] Del Valle, Y. et.al. Particle swarm optimization: Basic concepts, variants and applications in power systems. IEEE Transaction Evolutionary Computation, 12 171-175. doi: 10.1109/TEVC.2007.896686 (2008).
[29] Gong, T., Wang, L. & Ma, Y. Evolutionary neural architecture search based on a modified particle swarm optimization. Int. J. Mach. Learn. & Cyber. 16, 7793–7808 https://doi.org/10.1007/s13042-025-02686-x (2025).